Paper 44

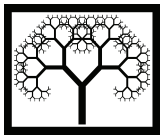

Proceedings of the Sixth International Conference
on Engineering Computational Technology,
M. Papadrakakis and B.H.V. Topping, (Editors),
Civil-Comp Press, Stirlingshire, Scotland

Parallel Computing Features of a Multiscale Strategy with Space and Time Homogenization

J.C. Passieux, P. Ladevèze and D. Néron
LMT-Cachan
ENS Cachan/CNRS/UPMC/PRES UniverSud Paris, France

Abstract

A new parallel and multiscale computational strategy for the analyze of heterogeneous structures has been proposed recently. This strategy includes automatic homogenization in space and time, with no periodicity condition and no condition on the scale ranges. It involves the resolution of a set of micro problems and a macro problem. In this paper, a new approximation for the resolution of micro problems is presented and applied to the multiscale strategy. The efficiency of the approach is examplified on a 3D test case.

Keywords: domain decomposition, time and space multiscale, LATIN, parallel computing.

1 Introduction

The behavior of large structures often results from complex phenomena taking place at a fine scale, with small length of variations both in space and time. For instance local cracking or local buckling have a global effect on large structures [1, 2, 15, 14, 19]. In order to predict the behavior of such structures, sophisticated models have been developed to describe the material at a very fine scale compared to the scale of the structure. Corresponding numerical simulations require the use of fine discretizations over both space and time domains, which often leads to systems with a very large number of degrees of freedom whose calculation cost is generally prohibitive.

Recently, a new multiscale computational strategy has been proposed for the analysis of such problems [11, 17, 16]. This strategy is based on the LArge Time INcrement method (LATIN method [18]), which enables one to work globally over the time-space domain. It can be seen as a parallel mixed domain decomposition strategy in space, including automatic space and time homogenization, and for which no pe-

riodicity condition is needed, in opposition with standard homogenization techniques [3, 4, 5, 6, 7].

The first idea consists in splitting the structure into substructures and interfaces, and dividing the studied time interval into subintervals. Interface fields are separated into a macro part and a micro complement. Thanks to the Saint-Venant's principle, an adapted choice of macro quantities, combined with the resolution of a global macro problem, ensures that micro quantities have only local effects. This choice provides to the method the numerical scalability with respect to space variables. A technique to extend this property to time aspects is in progress. The second idea consists in using an iterative technique involving the resolution of a set of independant problems on the refined "micro" scale and the resolution of a few problems on the homogenized "macro" scale. A new approximation technique for the resolution of micro problems is presented. It leads to drastic saving in terms of computation cost.

A 3D numerical example, with (visco)plastic material and unilateral contact with friction is provided to show the performances of the strategy combined with the new approximation technique, and to highlight the parallel properties.

2 The reference problem

In this Section, a brief review of the main aspects of the multiscale computational strategy is presented. Further details can be found in [18, 17, 16].

2.1 Description of the problem

Under the assumption of small perturbations, let us consider the quasi-static and isothermal evolution of a structure defined in the time-space domain $[0, T] \times \Omega$. This structure is subjected to prescribed body forces $\underline{f}_d$, to traction forces $\underline{F}_d$ over a part $\partial_2\Omega$ of the boundary, and to prescribed displacements $\underline{U}_d$ over the complementary part $\partial_1\Omega$ (see Figure 1). The displacement, strains and stresses are subjected to initial conditions at $t = 0$.

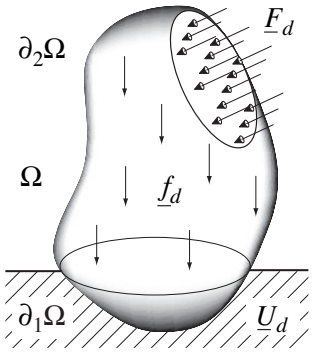

Figure 1: The reference problem

2.2 Constitutive relation model with internal state variables

$\boldsymbol{\sigma}$ designates the Cauchy stress field. $\boldsymbol{\varepsilon}_{\mathrm{p}}$ the inelastic part of the strain field $\boldsymbol{\varepsilon}$, is treated independently of the other internal variables, which are denoted by $\mathbf{X}$. The conjugate variables of $\mathbf{X}$ is $\mathbf{Y}$.

Introducing the following notations:

$$\mathbf{e}_{\mathrm{p}} = \begin{bmatrix} \boldsymbol{\varepsilon}_{\mathrm{p}} \\ -\mathbf{X} \end{bmatrix}, \ \mathbf{e} = \begin{bmatrix} \boldsymbol{\varepsilon} \\ 0 \end{bmatrix} \text{ and } \mathbf{e}_{\mathrm{e}} = \begin{bmatrix} \boldsymbol{\varepsilon}_{\mathrm{e}} \\ \mathbf{X} \end{bmatrix} \qquad \text{and} \qquad \mathbf{f} = \begin{bmatrix} \boldsymbol{\sigma} \\ \mathbf{Y} \end{bmatrix} \tag{1}$$

the mechanical dissipation rate for the entire structure Ω is:

$$\int_{\Omega} (\dot{\mathbf{e}}_{\mathrm{p}} \circ \mathbf{f}) d\Omega = \int_{\Omega} (\dot{\boldsymbol{\varepsilon}}_{\mathrm{p}} : \boldsymbol{\sigma} - \dot{\mathbf{X}} \cdot \mathbf{Y}) d\Omega \tag{2}$$

From the free energy $\rho\Psi(\boldsymbol{\varepsilon}_{\mathrm{e}}, \mathbf{X})$, under the usual uncoupling assumptions, one obtains the "normal" formulation of the state equation [18]:

$$\boldsymbol{\sigma} = \rho \frac{\partial \psi}{\partial \boldsymbol{\varepsilon}_{\mathrm{e}}} = \mathbf{K}\boldsymbol{\varepsilon}_{\mathrm{e}} \qquad \text{and} \qquad \mathbf{Y} = \rho \frac{\partial \psi}{\partial \mathbf{X}} = \boldsymbol{\Lambda}\mathbf{X} \tag{3}$$

where the Hooke's tensor $\mathbf{K}$ and the constant, symmetric and positive definite tensor $\boldsymbol{\Lambda}$ are material characteristics. These equations can be rewritten in the form:

$$\mathbf{f} = \mathbf{A}\mathbf{e}_{\mathrm{e}} \quad \text{with} \quad \mathbf{A} = \begin{bmatrix} \mathbf{K} & 0 \\ 0 & \boldsymbol{\Lambda} \end{bmatrix} \tag{4}$$

where $\mathbf{A}$ is a constant, symmetric and positive definite operator.

The constitutive equation is given by the positive differential operator $\mathbf{B}$, which is considered to be derived from the dissipation pseudo-potential $\phi^*(\boldsymbol{\sigma}, \mathbf{Y})$:

$$\dot{\mathbf{e}}_{\mathrm{p}} = \begin{bmatrix} \partial_{\boldsymbol{\sigma}} \phi^* \\ \partial_{\mathbf{Y}} \phi^* \end{bmatrix} = \mathbf{B}(\mathbf{f}) \quad \text{with} \quad \mathbf{e}_{\mathrm{p}|t=0} = 0 \tag{5}$$

2.3 Decomposition of the structure into substructures and interfaces

The structure is viewed as an assembly of simple components, i.e. substructures and interfaces, each with its own variables and equations [18, 10] (see Figure 2).

Each substructure Ω_E of Ω is subjected to the action of its neighboring interfaces, described by a displacement distribution $\underline{W}_E$ and a force distribution $\underline{F}_E$. Let $\Phi_{EE'}$ denote the interface between Ω_E and $\Omega_{E'}$. This interface is characterized by the restrictions to $\Phi_{EE'}$ of both the displacement field $(\underline{W}_E, \underline{W}_{E'})$ and the force field $(\underline{F}_E, \underline{F}_{E'})$, denoted $(\underline{W}_{EE'}, \underline{W}_{E'E})$ and $(\underline{F}_{EE'}, \underline{F}_{E'E})$ respectively. At Interface $\Phi_{EE'}$, the action-reaction principle:

$$\underline{F}_{EE'} + \underline{F}_{E'E} = \underline{0} \tag{6}$$

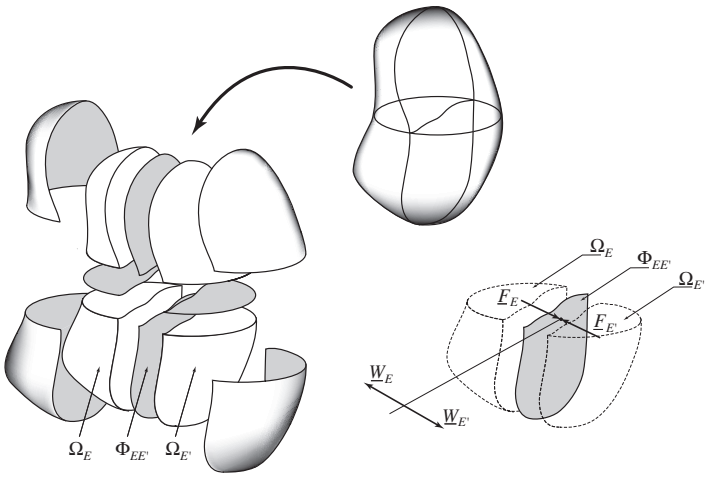

Figure 2: Decomposition of the structure into substructures and interfaces

holds, along with a constitutive relation of the form:

$$\underline{F}_{EE'|t} = \mathbf{b}_{EE'}\left(\left[\dot{\underline{W}}_{EE'} - \dot{\underline{W}}_{E'E}\right]_{|\tau}, \tau \leqslant t\right) \tag{7}$$

where $\mathbf{b}_{EE'}$ is an operator characterizing the behavior of the interface, of which the boundary conditions on $\partial_1\Omega$ and $\partial_2\Omega$ are particular cases. Example of such operator can be found in [11, 16].

2.4 Admissibility conditions for Substructure Ω_E

The following spaces are introduced. Notation $\square^\star$ is used for the corresponding vector space.

- The kinematic admissibility of displacement field set $(\underline{U}_E, \underline{W}_E)$:

$$(\underline{U}_E, \underline{W}_E) \in \mathcal{U}_E \quad \Longleftrightarrow \quad \underline{U}_{E|\partial\Omega_E} = \underline{W}_E \quad \text{and} \quad \underline{U}_{E|t=0} = \underline{U}_{E0} \tag{8}$$

- The static admissibility of stress field $\boldsymbol{\sigma}_E$:

$$\begin{aligned}\mathbf{f}_E = [\boldsymbol{\sigma}_E\ \mathbf{Y}_E]^T \in \boldsymbol{\mathcal{F}}_E \qquad &\Longleftrightarrow \\ \forall(\underline{U}^\star_E, \underline{W}^\star_E) \in \mathcal{U}^\star_E, \quad &-\int_{[0,T]\times\Omega_E} \boldsymbol{\sigma}_E : \boldsymbol{\varepsilon}(\dot{\underline{U}}^\star_E) d\Omega dt \\ &+ \int_{[0,T]\times\Omega_E} \underline{f}_d \cdot \dot{\underline{U}}^\star_E d\Omega dt + \int_{[0,T]\times\partial\Omega_E} \underline{F}_E \cdot \dot{\underline{W}}^\star_E dS dt = 0\end{aligned} \tag{9}$$

- The kinematic admissibility of the strain rate field $\dot{\boldsymbol{\varepsilon}}_E$:

$$\begin{aligned}\mathbf{e}_E = [\dot{\boldsymbol{\varepsilon}}_E\ -\dot{\mathbf{X}}_E]^T \in \boldsymbol{\mathcal{E}}_E \qquad &\Longleftrightarrow \qquad \forall(\mathbf{f}^\star_E, \underline{F}^\star_E) \in \boldsymbol{\mathcal{F}}^\star_E, \\ &-\int_{[0,T]\times\Omega_E} \boldsymbol{\sigma}^\star_E : \dot{\boldsymbol{\varepsilon}}_E d\Omega dt + \int_{[0,T]\partial\Omega_E} \underline{F}^\star_E \cdot \dot{\underline{W}}_E dS dt = 0\end{aligned} \tag{10}$$

Finally, we denote by $\mathbf{A}_{\mathbf{d}E}$ the space of the set of "E-admissible" variables $\mathbf{s}_E = (\dot{\mathbf{e}}_{\mathrm{p}E}, \underline{\dot{W}}_E, \mathbf{f}_E, \underline{F}_E)$ which verify:

$$(\mathbf{A}^{-1}\dot{\mathbf{f}}_E + \dot{\mathbf{e}}_{\mathrm{p}E}) \in \boldsymbol{\mathcal{E}}_E \quad \text{and} \quad \mathbf{f}_E \in \boldsymbol{\mathcal{F}}_E \tag{11}$$

2.5 Formulation of the reference problem

Then the decomposed reference problem, defined over the entire time-space domain $[0,T] \times \Omega$, can be formulated as follows:

Find $\mathbf{s}_{\mathbf{ref}} = (\mathbf{s}_E)_{\Omega_E \subset \Omega}$ which verifies, $\forall \Omega_E \subset \Omega$,

- the E-admissibility condition $\quad \mathbf{s}_E \in \mathbf{A}_{\mathbf{d}E}$
- the evolution law $\quad \dot{\mathbf{e}}_{\mathrm{p}E} = \mathbf{B}(\mathbf{f}_E) \quad \text{with} \quad \mathbf{e}_{\mathrm{p}E_{|t=0}} = 0$
- the interface behavior $\quad \forall \Omega_{E'} \in \boldsymbol{\Omega}_E,\ \underline{F}_{EE'} + \underline{F}_{E'E} = \underline{0} \quad \text{and}$

$$\underline{F}_{EE'|t} = \mathbf{b}_{EE'}\left(\left[\underline{\dot{W}}_{EE'} - \underline{\dot{W}}_{E'E}\right]_{|\tau}, \tau \leqslant t\right) \tag{12}$$

3 Multiscale description in the time-space domain

3.1 A two-scale description of the unknowns

The approach consists in introducing a two-scale description of the unknowns: these two scales are denoted "macro" ($\square^M$) and "micro" ($\square^m$) and concern both space and time. The distinction between the macrolevel and the microlevel is made only at the interfaces.

Spaces $\mathcal{W}_E^M$ and $\mathcal{F}_E^M$ of macro quantities can be chosen arbitrarily. Once these spaces have been chosen, the macro part $\underline{\dot{W}}_E^M$ of Field $\underline{\dot{W}}_E \in \mathcal{W}_E$ is defined by the best approximation in the sense of the work's bilinear form [16]. And then the micro complements are $\underline{\dot{W}}_E^m = \underline{\dot{W}}_E - \underline{\dot{W}}_E^M$ and $\underline{F}_E^m = \underline{F}_E - \underline{F}_E^M$, and the scales are uncoupled as follows:

$$\int_{[0,T]\times\partial\Omega_E} \underline{\dot{W}}_E \cdot \underline{F}_E dSdt = \int_{[0,T]\times\partial\Omega_E} (\underline{\dot{W}}_E^M \cdot \underline{F}_E^M + \underline{\dot{W}}_E^m \cdot \underline{F}_E^m) dSdt \tag{13}$$

For space, the macroscale is defined by the characteristic length of the interfaces. Classically, the macro parts are defined as affine functions on each interface $\Phi_{EE'}$. For time, the macroscale is associated with a coarse partition $\mathcal{T}_h^M = \{0 = t_0^M, \ldots, t_{n^M}^M = T\}$ of the time interval $[0,T]$ being studied. Classically, the macro parts are defined as polynomials of degree p in each macro interval $I_k^M =]t_k^M, t_{k+1}^M[$. Let us note that the choice of functions which are possibly discontinuous implies that one should consider all the equations in the time-discontinuous Galerkin scheme sense [8].

The choices adopted for the definition of the macro quantities are physically sound: these quantities are mean values in time and in space.

3.2 Admissibility of the macro quantities

An important point of the multiscale computational strategy is the choice of the admissibility conditions for the macro quantities. The set of the macro forces $\underline{F}^M = (\underline{F}^M_E)_{\Omega_E \subset \Omega}$ is required, *a priori*, to verify the transmission conditions systematically, including the boundary conditions. The corresponding subspace of $\mathcal{F}^M$ is designated by $\mathcal{F}^M_{\mathbf{ad}}$. The subspace of $\mathcal{F}$ whose elements have their macro parts in $\mathcal{F}^M_{\mathbf{ad}}$ is designated by $\mathcal{F}_{\mathbf{ad}}$.

4 The multiscale computational strategy

4.1 The engine of the strategy

The *a priori* partial verification of the transmission conditions at the interfaces leads to the following reformulation of the reference problem: find $\mathbf{s_{ref}} = (\mathbf{s}_E)_{\Omega_E \subset \Omega}$ which verifies, $\forall \Omega_E \subset \Omega$,

$$\begin{array}{rll} \mathbf{A_d} & \left\| \begin{array}{ll} \text{(a)} & \text{the } E\text{-admissibility condition } \mathbf{s}_E \in \mathbf{A_d}E \\ \text{(b)} & \text{the admissibility of the macro forces} \end{array} \right. & \\ \boldsymbol{\Gamma} & \left\| \begin{array}{ll} \text{(c)} & \text{the state evolution law} \\ \text{(d)} & \text{the interface behavior} \end{array} \right. & \end{array} \tag{14}$$

The engine of the strategy is the LATIN method [18], a general computational strategy for time dependent non linear problems with the particularity to be an iterative strategy which operates globally over the space-time domain (see for example an application to discrete media [13]). The first principle of the LATIN method consists in dealing with the difficulties separately by dividing the solutions of the equations into two independent subspaces: the space $\mathbf{A_d}$ of the solutions to the global linear equations (14a) and (14b) and the space $\boldsymbol{\Gamma}$ of the solutions to the local nonlinear equations (14c) and (14d).

To close this problem the LATIN proposes to introduce what we call the search directions, and the corresponding iterative scheme which consists in building fields of $\boldsymbol{\Gamma}$ and $\mathbf{A_d}$ alternatively. The exact solution trivially belongs to their intersection $\mathbf{s_{ref}} = \mathbf{A_d} \cap \boldsymbol{\Gamma}$. The Figure 3 shows the geometrical interpretation of one iteration made of two stages called the "local stage" and the "linear stage".

4.2 The local stage at Iteration $n+1$

This stage consists in building $\hat{\mathbf{s}}_{n+1/2} \in \boldsymbol{\Gamma}$ knowing $\mathbf{s}_n \in \mathbf{A_d}$ and using the search direction $\mathbf{E}^+$, followed by $\hat{\mathbf{s}}_{n+1/2} - \mathbf{s}_n = D\mathbf{s}$ (see Figure 3). This search direction is local in space because the sought fields have no constraints. It is defined by:

$$\left\{ \begin{array}{c} D\dot{\mathbf{e}}_{\mathrm{p}E} + \mathbf{H}D\mathbf{f}_E = 0 \\ D\dot{\underline{W}}_E - \mathbf{h}D\underline{F}_E = 0 \end{array} \right. \tag{15}$$

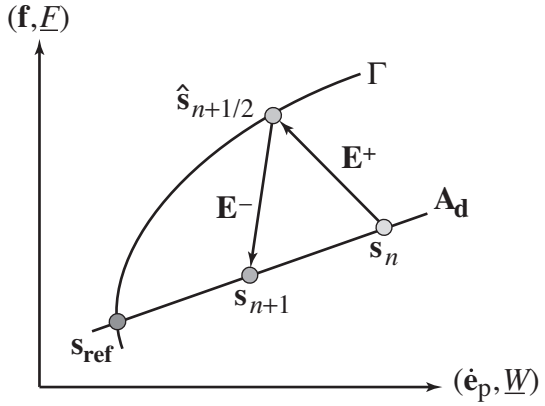

Figure 3: Iteration $n+1$ of the LATIN method

where $\mathbf{H}$ and $\mathbf{h}$ are symmetric, positive definite operators which are parameters of the method. This stage leads to the resolution of a set of problems which are local—*i.e.* on each point of the discretization—in the space and time variables, and therefore, lend themselves to the highest degree of parallelism.

4.3 The linear stage at Iteration $n+1$

This stage consists in building $\mathbf{s}_{n+1} \in \mathbf{A_d}$ knowing $\hat{\mathbf{s}}_{n+1/2} \in \mathbf{\Gamma}$ and using the search direction $\mathbf{E}^-$, followed by $\mathbf{s}_{n+1} - \hat{\mathbf{s}}_{n+1/2} = D\mathbf{s}$ (see Figure 3). The substructure part of the search direction is defined by:

$$D\dot{\mathbf{e}}_{\mathrm{p}E} - \mathbf{H}D\mathbf{f}_E = 0 \tag{16}$$

Because of the admissibility of the macro forces, the boundary part of the search direction can be redefined using a weak formulation, introducing a Lagrange multiplier $\underline{\dot{\tilde{W}}}_E^M$ to guarantee the admissibility of the macro forces in a week sense: $\underline{\dot{\tilde{W}}}^M$ ($\underline{\dot{\tilde{W}}}^M = (\underline{\dot{\tilde{W}}}_E^M)_{\Omega_E \subset \Omega} \in \mathcal{W}_{\mathbf{ad}}^{M\star}$):

$$\forall \underline{F}^\star \in \mathcal{F}, \sum_{\Omega_E \subset \Omega} \left\{ \int_{[0,T]\times\partial\Omega_E} (D\underline{\dot{W}}_E + \mathbf{h}D\underline{F}_E - \underline{\dot{\tilde{W}}}_E^M) \cdot \underline{F}_E^\star dSdt \right\} = 0 \tag{17}$$

and the admissibility of the macro forces is expressed by:

$$\forall \underline{\dot{\tilde{W}}}^{M\star} \in \mathcal{W}_{\mathbf{ad}}^{M\star}, \sum_{\Omega_E \subset \Omega} \left\{ \int_{[0,T]\times\partial\Omega_E} \underline{\dot{\tilde{W}}}_E^{M\star} \cdot (\underline{F}_E - \underline{F}_d)\, dSdt \right\} = 0 \tag{18}$$

The resolution of the linear stage can be divided into two parts. The resolution of a set of micro problems defined over each time-space substructure $[0,T] \times \Omega_E$, and the resolution of a global macro problem defined over the entire time-space domain $[0,T] \times \Omega$.

4.3.1 The micro problems defined over each $[0,T]\times\Omega_E$ and $[0,T]\times\partial\Omega_E$

Each micro problem associated with Ω_E is a linear evolution equation:

$$\begin{array}{l}\text{Find } (\mathbf{s}_E)_{\Omega_E\subset\Omega} \text{ which verifies, } \forall\Omega_E\subset\Omega,\\ \bullet\ \text{the } E\text{-admissibility condition} \quad \mathbf{s}_E\in\mathbf{A}_{\mathbf{d}E}\\ \bullet\ \text{the search direction} \quad (16,17)\end{array} \tag{19}$$

Since (17) is local at Boundary $\partial\Omega_E$, the micro problems in the substructures are independent of one another. Since $\mathbf{H}$ and $\mathbf{h}$ are positive definite operators, the micro problem defined over $[0,T]\times\Omega_E$ has a unique solution such that:

$$\mathbf{s}_E=\mathbf{s}_E^{(1)}+\mathbf{s}_E^{(2)}(\dot{\underline{\tilde{W}}}_E^M) \tag{20}$$

where $\mathbf{s}_E^{(1)}$ depends on the additional loading and on the previous approximation of the solution $\hat{\mathbf{s}}_E$, and $\mathbf{s}_E^{(2)}$ depends linearly on $\dot{\underline{\tilde{W}}}_E^M$, which is unknown at this stage. In particular, one has:

$$\underline{F}_E^M=\hat{\underline{F}}_{E,d}^M+\mathbf{L}_E\dot{\underline{\tilde{W}}}_E^M \tag{21}$$

where $\hat{\underline{F}}_{E,d}$ is due to the additional loading and to the previous approximation to the solution, and $\mathbf{L}_E$ is a linear operator which can be interpreted as a homogenized behavior operator over the time-space substructure $[0,T]\times\Omega_E$. This operator can be calculated by solving a set of micro problems over $[0,T]\times\Omega_E$ in which one takes successively for $\dot{\underline{\tilde{W}}}_E^M$ the macro basis functions of $\mathcal{W}_E^M$. The calculation of those operators can be driven in parallel in space as well as in time.

4.3.2 The macro problem defined over $[0,T]\times\Omega$

The macro problem defined over the entire time-space domain $[0,T]\times\Omega$ is:

$$\begin{array}{l}\text{Find } (\dot{\underline{\tilde{W}}}^M,\underline{F}^M) \text{ which verifies :}\\ \bullet\ \text{the admissibility of the Lagrange multiplier} \quad \dot{\underline{\tilde{W}}}^M\in\mathcal{W}_{\mathbf{ad}}^{M\star}\\ \bullet\ \text{the admissibility of the macro forces} \quad \underline{F}\in\mathcal{F}_{\mathbf{ad}}\\ \bullet\ \text{the homogenized behavior} \quad (21)\end{array} \tag{22}$$

Introducing (21) into the admissibility condition of the macro forces (18), and using the micro-macro uncoupling property (13), one has:

$$\forall\dot{\underline{\tilde{W}}}^{M\star}\in\mathcal{W}_{\mathbf{ad}}^{M\star},\ \sum_{\Omega_E\subset\Omega}\left\{\int_{[0,T]\times\partial\Omega_E}\dot{\underline{W}}_E^{M\star}\cdot(\hat{\underline{F}}_{E,d}^M+\mathbf{L}_E\dot{\underline{\tilde{W}}}_E^M)dSdt - \int_{[0,T]\times\Phi_{E2}}\dot{\underline{\tilde{W}}}_E^{M\star}\cdot\underline{F}_d dSdt\right\}=0 \tag{23}$$

which corresponds to the resolution of a homogenized problem over the whole structure.

4.3.3 Resolution of the linear stage

The resolution of the linear stage proceeds as follows: first, one solves a set of micro problems, each defined over $[0,T] \times \Omega_E$, in which one takes into account only the data $\hat{\mathbf{s}}_E$ of the previous stage. This leads to $\mathbf{s}_E^{(1)}$. Then, one solves the macro problem defined over $[0,T] \times \Omega$, leading to $\underline{\dot{\tilde{W}}}^M$. Finally, in order to obtain $\mathbf{s}_E^{(2)}$, one solves a second series of micro problems with the Lagrange multiplier as the only data.

Since the macro mesh is defined in time and in space, the micro problems are independent not only from one substructure to another, but also from one macro time interval to another.

4.4 Convergence of the algorithm

Since the reference solution $\mathbf{s_{ref}}$ is the intersection of $\mathbf{\Gamma}$ and $\mathbf{A_d}$, the distance between $\hat{\mathbf{s}}_{n+1/2}$ and $\mathbf{s}_n$ is a good error indicator to verify the convergence of the algorithm. The simplest measure of this distance is:

$$\eta = \frac{\|\hat{\mathbf{s}}_{n+1/2} - \mathbf{s}_n\|}{\frac{1}{2}\|\hat{\mathbf{s}}_{n+1/2} + \mathbf{s}_n\|} \tag{24}$$

with:

$$\|\mathbf{s}\|^2 = \frac{1}{2} \sum_{\Omega_E \subset \Omega} \int_{[0,T]\times\Omega_E} (1 - \frac{1}{T})(\dot{\mathbf{e}}_{\mathrm{p}E} \circ \mathbf{H}^{-1}\dot{\mathbf{e}}_{\mathrm{p}E} + \mathbf{f}_E \circ \mathbf{H}\mathbf{f}_E) d\Omega dt \tag{25}$$

Finally, the algorithm can be summed up as follows:

Algorithm 1: Algorithm of the strategy (// =parallel stage)

Initialisation: $\mathbf{s}_0 \in \mathbf{A}_d$
for $n = 1$ ***to*** n_{max} **do**
  Local stage
    // • Local problems on the substructures Ω_E
    // • Local problems on the interfaces $\Gamma_{EE'}$
  Linear stage
    // • Linear problems defined on $\Omega_E \times [0,T]$
    • 1 macro linear problem defined on $\Omega_E \times [0,T]$
    // • Linear problems defined on $\Omega_E \times [0,T]$
  Error indicator
end

4.5 Scalability

Let us remind that Spaces $\mathcal{W}_E^M$ and $\mathcal{F}_E^M$ can be chosen arbitrarily. In the aim of being numerically scalable, we classically use a space macro basis which allow to extract

the linear part of the interface forces and displacements. This choice has a strong mechanical meaning, since the macro part of the effort includes the resultants forces and moments. Then the micro complements, thanks to the Saint Venant's principle only have a local effect. With such a choice, the resultants of the forces are in equilibrium through the whole structure at each iteration thanks to the resolution of the macro problem. Then the micro complement is localized on the neighborhood of the interface. This property reduces the dependences between the micro problems on each substructures.

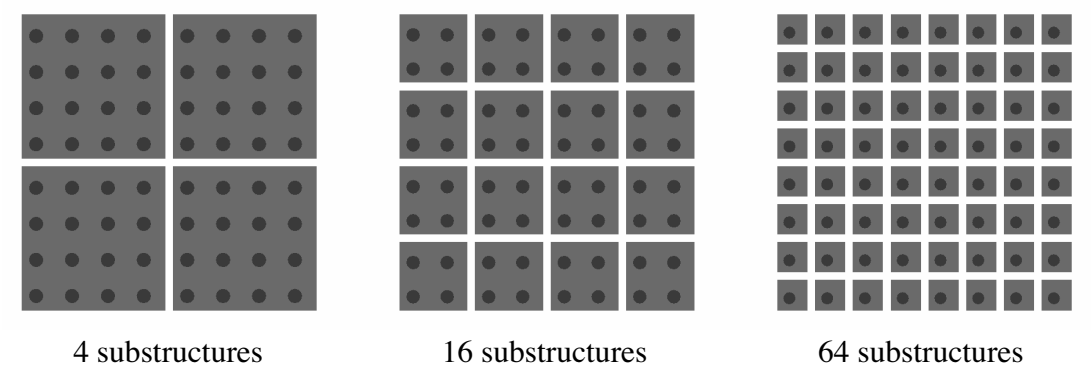

Figure 4: Three different decompositions of the problem

To examplify the scalability property, let us consider an example of a 2D viscoelastic heterogeneous structure clamped at the bottom and subjected to a traction force at the top. We study the influence of the number of substructures on the convergence rate of the strategy. Three different decompositions are given in Figure 4. In space, the macro basis is made of four functions—two translations, one rotation and one extension for the displacement;two resultants forces, one resultant moment, and one extension for the forces— In time, the micro and macro scales are chosen, in this case, to be the same.

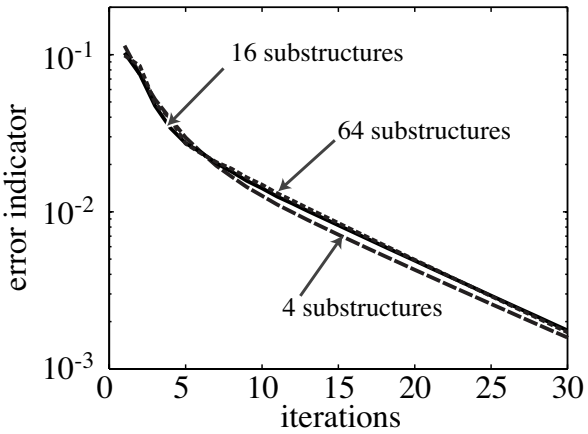

Figure 5: Convergence rates corresponding to the three different decompositions

On Figure 5 we represent the evolution of the error indicator η of the strategy throughout the iterations of the algorithm. One can notice that the three decompositions drive to the same convergence rate. This property, associated with the fact that almost every stages of the strategy are parallel—except for the macro problem, which is reduced on a few degrees of freedom (DOFs) by interfaces—allow us to say that the strategy is scalable. Efficiency and speedup only depend on the computation cost of the macro problem compared to the cost of the resolution of the set of micro problems. According to our tests, the resolution of the macro problem is often cheap compared to the one of the micro problems. However, if the number of macro time-space substructures is large, an approximation technique based on the introduction of a third scale can be used [11]. The macro problem can also be parallelized, for an optimal efficiency.

Concerning time aspects, in some cases, non-full scalability has been noticed. A technique based on macro time base enrichment is in progress.

4.6 Example

Let us consider the 3D problem of a composite structure containing cracks (see Figure 6(a)). The structure is clamped at the bottom and subjected to forces $\underline{F}_1$, $\underline{F}_3$ and $\underline{F}_3$ (see Figure 6(b)). The overall dimensions are $120 \times 120 \times 20$ mm, and the time interval being studied is $T = 10$ s. The cracks are described using unilateral contact with Coulomb friction characterized by Parameter $f = 0.3$.

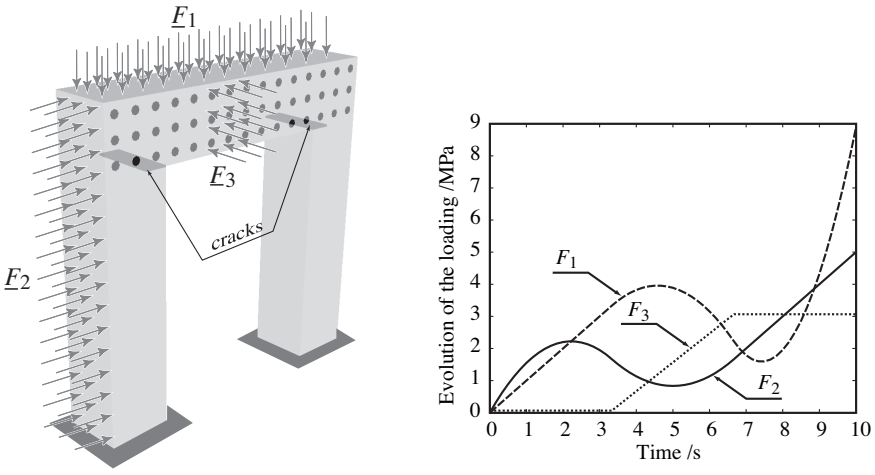

(a) Geometry and loading

(b) Loads $\underline{F}_1$, $\underline{F}_3$ and $\underline{F}_3$

Figure 6: Description of the problem

The structure consists of two types of cells: Type-I cells are homogeneous, made of Type-1 material; Type-II cells consist of a matrix of Type-1 material with inclusions of Type-2 material. Type-1 and Type-2 materials are viscoelastic and their properties are given in Table 1. The corresponding constitutive relations are $\dot{\boldsymbol{\varepsilon}}_p = \mathbf{B}_i\boldsymbol{\sigma} = \frac{1}{\eta_i}\mathbf{K}_i^{-1}\boldsymbol{\sigma}$.

Material	Type-1	Type-2
Young's modulus	$E_1 = 50$ GPa	$E_2 = 250$ GPa
Poisson's ratio	$\nu_1 = 0.3$	$\nu_2 = 0.2$
Viscosity parameter	$\eta_1 = 10$ s	$\eta_2 = 1000$ s

Table 1: Material properties

The problem was divided into 351 substructures and 1,296 interfaces as shown on Figure 7, each substructure corresponding to one cell. On the microlevel, Type-I and Type-II substructures and interfaces were meshed with 847, 717 and 144 DOFs respectively. The macro part consisted of a single linear element with only 9 DOFs per interface. With respect to time, the microlevel was associated with a refined discretization into 60 intervals using a zero-order discontinuous Galerkin scheme, and the macrolevel was associated with a coarse discretization into 3 macro intervals using a second-order discontinuous Galerkin scheme.

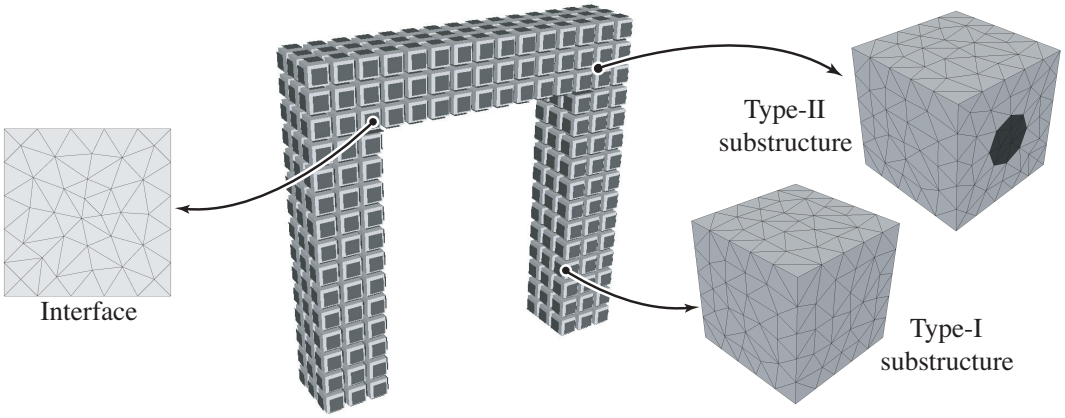

Figure 7: Decomposition and microscale discretizations in space

Since, here, the state evolution law is linear, the search direction chosen for the substructures was $\mathbf{H} = \mathbf{B}$. The characteristic length of the interfaces being $L_E = 4$ mm, we chose for all the interfaces the search direction $\mathbf{h} = h\mathbf{I}$, where $h = \frac{L_E}{E_1 \nu_1}$ is a constant scalar.

Figure 8 shows the evolution of the error indicator η throughout the iterations. One can observe that the algorithm converges rapidly toward an accurate solution (1% error after 12 iterations).

An example of the micro/macro description of the solution is given in Figure 9. Figures 9(a) and 9(b) show the evolutions of Force $\underline{F}$ and its macro part $\underline{F}^M$ respectively at time $t = 2/3T$ over a horizontal line L_1 in the heterogeneous part of the structure, and as functions of time at a point P_1 of the previous line. Figures 9(a) and 9(b) show the same evolutions for Displacement $\underline{W}$ and its macro part $\underline{W}^M$.

One can observe that the macro part of the quantities being considered constitutes a good average approximation of the solution, obtained with only a very small number

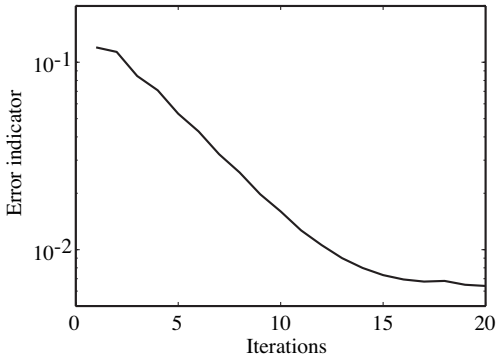

Figure 8: Convergence of the method

of basis functions (27 DOFs per interface and per macro interval). The choice of such a basis leads to the resolution at each iteration of a macro problem with a strong mechanical meaning and with only a few DOFs (in this example, 35,000 DOFs compared to 270,000 DOFs for the assembled reference problem).

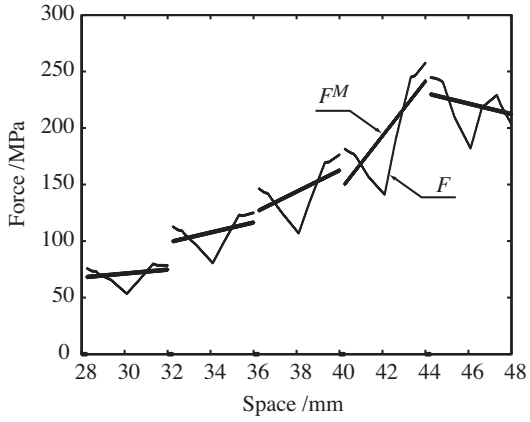

(a) $\underline{F}$ and $\underline{F}^M$ at $t = 2/3T$ over Line L_1

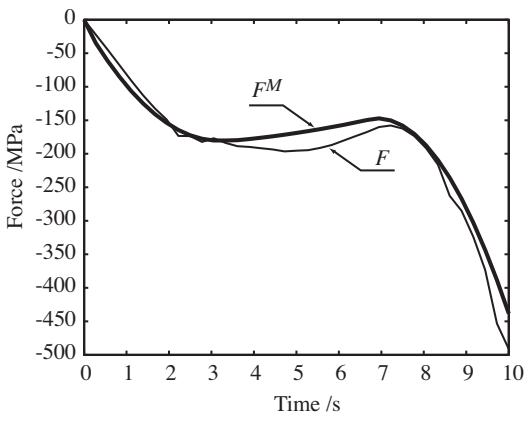

(b) $\underline{F}$ and $\underline{F}^M$ at Point P_1 as functions of time

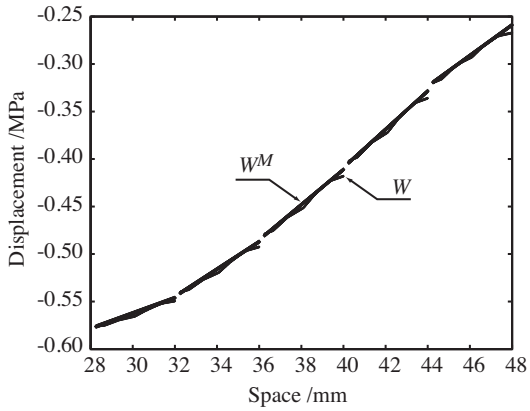

(c) $\underline{W}$ and $\underline{W}^M$ $t = 2/3T$ over Line L_1

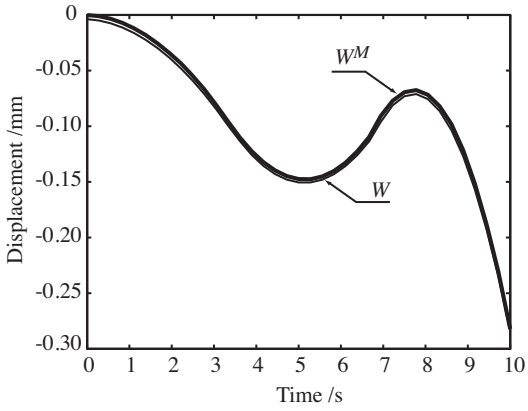

(d) $\underline{W}$ and $\underline{W}^M$ at Point P_1 as functions of time

Figure 9: Micro/macro description of the solution

5 The new radial time-space approximation

Throughout the iterative process, one has to solve for each of the substructures a set of micro problems defined on $[0,T] \times \Omega$, which can can vary only slightly from an iteration to the other. The standard methods do not take advantage of this property, therefore their costs can be prohibitive. This is what led the development of what we call the "radial time-space approximation".

The radial time-space approximation was introduced by Ladevèze in (see [9], and also [18]) and is part of the LATIN method. The basic idea consists in approximating a function f defined over the time-space domain $[0,T] \times \Omega$ by a finite sum of products of time functions λ_i by space functions Λ_i:

$$\forall (t,M) \in [0,T] \times \Omega, \quad f(t,M) : \sum_i \lambda_i(t) \Lambda_i(\underline{M}) \tag{26}$$

where the products $\lambda_i(t)\Lambda_i(\underline{M})$ are called "radial time-space functions". It is important to note that this is not a spectral decomposition because neither the λ_i nor the Λ_i are known *a priori*.

5.1 Rewriting of a micro problem over $[0,T] \times \Omega_E$

In this part, we rewrite the linear stage as a problem of minimization, in which the approximation will be introduced.

For each $[0,T] \times \Omega_E$, the search direction (16) can be interpreted as a linear constitutive relation. Thus, an equivalent formulation consists in minimizing the global constitutive relation error in $\mathbf{A}^{\star}_{\mathbf{d}E}$, which is defined over the time-space substructure $[0,T] \times \Omega_E$. Then, the linear stage consists in finding $\mathbf{s}_{E,n+1} \in \mathbf{A}_{\mathbf{d}E}$ which minimizes the constitutive relation error $e^2_{CR,E}(\mathbf{s}_{E,n+1} - \hat{\mathbf{s}}_{E,n+1/2}) = e^2_{CR,E}(D\mathbf{s}_E)$ associated with the search direction, defined by:

$$e^2_{CR,E}(D\mathbf{s}_E) = \|D\dot{\mathbf{e}}_E - \mathbf{H}D\mathbf{f}_E\|^2_{\mathbf{H},E} + \left\|D\dot{\underline{W}}_E + \mathbf{h}D\underline{F}_E\right\|^2_{\mathbf{h},E} \tag{27}$$

where the corresponding norms are:

$$\|\square\|^2_{\mathbf{H},E} = \int_{[0,T]\times\Omega_E} (1 - \frac{t}{T})\square \circ \mathbf{H}^{-1}\square d\Omega dt \tag{28}$$

and:

$$\|\square\|^2_{\mathbf{h},E} = \int_{[0,T]\times\partial\Omega_E} (1 - \frac{t}{T})\square \cdot \mathbf{h}^{-1}\square dS dt \tag{29}$$

Let us notice, that if we find an approximation of this problem, the only equation that will not be exactly verified is the search direction which is a parameter of the method, and which has an effect on the convergence rate only. According to our test, even with a coarse verification of the search direction, the effect on the convergence rate is rather slight.

5.2 Introduction of the approximation

The solution of the linear stage at iteration $n+1$ can be written as an incremental correction $\Delta\mathbf{s}$ to the previous approximation $\mathbf{s}_n$, namely $\mathbf{s}_{n+1} = \mathbf{s}_n + \Delta\mathbf{s}$. Knowing $\mathbf{s}_n$, at Iteration $n+1$, we choose to compute the approximation of Correction $\Delta\mathbf{s}$ only.

The choice of the approximation presented herein is an improvement over the version introduced in [12]. The starting point is the introduction as unknowns of the radial time-space approximations of the corrections related to the inelastic strain and to the additional internal variables:

$$\begin{aligned} \Delta\boldsymbol{\varepsilon}_{\mathrm{p}E}(t,\underline{M}) &= \sum_{k=1}^{p} a^k(t)\mathbf{E}^k_{\mathbf{p}}(\underline{M}) \\ \Delta\mathbf{X}_E(t,\underline{M}) &= \sum_{k=1}^{p'} b^k(t)\mathbf{D}^k(\underline{M}) \end{aligned} \tag{30}$$

Using the E-admissibility conditions, one determines the other quantities of interest in terms of the previous unknowns:

$$\begin{aligned} (\Delta\boldsymbol{\varepsilon}_E, \Delta\underline{W}_E)(t,\underline{M}) &= \sum_{k=1}^{p} a^k(t)(\mathbf{E}^k, \underline{Z}^k)(\underline{M}) \\ (\Delta\boldsymbol{\sigma}_E, \Delta\underline{F}_E)(t,\underline{M}) &= \sum_{k=1}^{p} a^k(t)(\mathbf{C}^k, \underline{G}^k)(\underline{M}) \\ \Delta\mathbf{Y}_E(t,\underline{M}) &= \sum_{k=1}^{p'} b^k(t)\mathbf{R}^k(\underline{M}) \end{aligned} \tag{31}$$

where the space functions are linked by the relations:

$$\mathbf{E}^k = \mathbf{E}^k_{\mathbf{p}} + \mathbf{K}^{-1}\mathbf{C}^k \quad \text{and} \quad \mathbf{R}^k = \boldsymbol{\Lambda}\mathbf{D}^k \tag{32}$$

and the space operators are defined through standard finite element approximation over the space domain Ω_E.

Compared to the previous version of the radial loading time-space approximation, we obtain the same quality of approximation with only half the number of time functions.

5.3 Definition of the best approximation

In order to solve (27), the idea is to seek minima alternatively with respect to time (which leads to a system of differential equations) and to space (which leads to a few "spatial" problems). Since the construction of the space functions is by far the most expensive step of this process, it is advantageous to store and reuse these functions. Thus, the space functions constructed up to Iteration n are reused systematically during Iteration $n+1$. Let us note that a reduced basis can be shared by several substructures if these substructures are similar.

5.4 Practical resolution technique

Let us assume that we are dealing with Iteration $n+1$ and that we have at our disposal a reduced basis made up of the space functions $\{(\mathbf{E}^k_{\mathbf{p}}, \mathbf{D}^k)\}_{k=1,\dots,m}$ for the approximation of the corrections related to the inelastic strain $\Delta\boldsymbol{\varepsilon}_{\mathrm{p}E}$ and to the additional internal variables $\Delta\mathbf{X}_E$. The space functions related to the other quantities $\Delta\boldsymbol{\varepsilon}_E$, $\Delta\underline{W}_E$, $\Delta\boldsymbol{\sigma}_E$ and $\Delta\underline{F}_E$ are also considered to be known.

Step 1: use of the reduced basis. One introduces the approximation into the constitutive relation error (27) where only the time functions are the unknowns. In other words, one seeks the best combination of the reduced basis of space functions which minimizes the constitutive relation error. These time functions verify a linear differential equation in time with conditions at $t = 0$ and $t = T$, whose solution is obtained classically. This is generally a rather small system. If the value of the constitutive relation error is small enough, one stops the process and selects the approximation obtained. Otherwise, one proceeds to *Step 2*.

Step 2: adding new functions. The previous approximation is considered to be known, and a new pair of time and space function is sought. One seeks a minimum alternatively over the time functions and the space functions. The minimization with respect to the space functions is standard, with twice the size of a classical finite element calculation, and which can easily be turned into the resolution of only a few sub-resolutions of classical finite element calculations, what is done in practice. The minimization with respect to the time functions leads to a differential equation with conditions at $t = 0$ and $t = T$, which can be easily solved using a standard technique. In practice, one stops after 1 or 2 subiterations.

6 Conclusions

The multiscale computational strategy with space and time homogenization was presented. The efficiency and the scalability of this approach make it well suited for parallel computing. The choice of macro basis has proved to be relevant. To extend the full scalability when micro and macro time are very different, a dedicated technique is under development. A new radial approximation technique for the resolution of the micro problems of the multiscale strategy has also been presented. This new technique involves the computation of approximately half the number of time functions needed by the previous approach. This technique not only reduces the number of computation of time functions, but increases its robustness. It also leads to the construction of a relevant basis of space functions, that can be reused along the iterations of the strategy. This new technique was implemented in a 3D viscoelastic code and mixed with the multiscale computational strategy.

References

[1] P.A. Guidault, O. Allix, L. Champaney and J.P. Navarro, *"A two-scale approach with homogenization for the computation of cracked structures"*, Computers & Structures, 85, 1360-1371, 2007

[2] P. Cresta and O. Allix and C. Rey and S. Guinard, *"Comparison of multiscale nonlinear strategies for post-buckling analysis"*, Computer Methods in Applied Mechanics and Engineering, 196, 1436-1446, 2007.

[3] E. Sanchez-Palencia, *"Non homogeneous media and vibration theory"*, Lecture Notes in Physics, 127, 1980.

[4] F Feyel, *"A multilevel finite element method (FE2) to describe the response of highly non-linear structures using generalized continua"*, Computer Methods in Applied Mechanics and Engineering, 192, 3233-3244, 2003.

[5] F. Devries and H. Dumontet and G. Duvaut and F. Léné, *"Homogenization and damage for composite structures"*, International Journal for Numerical Methods in Engineering, 27, 285-298, 1989.

[6] J. T. Oden and K. Vemaganti and N. Moës, *"Hierarchical modeling of heterogeneous solids"*, Computer Methods in Applied Mechanics and Engineering, 172, 3-25, 1999.

[7] J. Fish, K. Shek, M. Pandheeradi, M. S. Shephard, *"Computational plasticity for composite structures based on mathematical homogenization: Theory and practice"*, Computer Methods in Applied Mechanics and Engineering, 148, 53-73, 1997.

[8] K. Eriksson, C. Johnson and V. Thomée, *"Time discretization of parabolic problems by the discontinuous galerkin formulation"*, RAIRO Modélisation Mathématique et Analyse Numérique, 19, 611-643, 1985.

[9] P. Ladevèze and P. Rougée, *"(Visco)plasticity under cyclic loadings: properties of the homogenized cycle"*, Comptes Rendus Académie des Sciences Paris (in french), II(301), 891-894, 1985.

[10] P. Ladevèze, O. Loiseau and D. Duresseix, *"A micro-macro and parallel computational strategy for highly heterogeneous structures"*, International Journal for Numerical Methods in Engineering, 52, 121-138, 2001.

[11] P. Ladevèze and A. Nouy, *"On a multiscale computational strategy with time and space homogenization for structural mechanics"*, Computer Methods in Applied Mechanics and Engineering, 192, 3061-3087, 2003.

[12] A. Nouy and P. Ladevèze, *"Multiscale computational strategy with time and space homogenization: a radial-type approximation technique for solving microproblems"*, International Journal for Multiscale Computational Engineering, 2, 557-574, 2004.

[13] P. Alart and D. Duresseix, *"A scalable multiscale LATIN method adapted to nonsmooth discrete media"*, Computer Methods in Applied Mechanics and Engineering, 197, 319-331, 2008.

[14] J. T. Oden, S. Prudhomme, A. Romkes, and P. T. Bauman, *"Multi-scale modeling of physical phenomena: Adaptative control of models"*, SIAM Journal for

Scientific Computing, 28, 2359-2389, 2006.

[15] A. Ibrahimbegovic and S. Melnyk, *"Embedded discontinuity finite element method for modeling of localized failure in heterogeneous materials with structured mesh: an alternative to the extended finite element method"*, Computational mechanics, 40, 149-155, 2007.

[16] P. Ladevèze, D. Néron and J.-C. Passieux, *"On multiscale computational mechanics with time-space homogenization"*, Textbook: Bridging the scales in Science and Engineering, Ed. J. Fish, to appear 2008.

[17] P. Ladevèze, D. Néron and P. Gosselet, *"On a mixed and multiscale domain decomposition method"*, Computer Methods in Applied Mechanics and Engineering, 196, 1526-1540, 2007.

[18] P. Ladevèze, *"Nonlinear Computational Structural Mechanics – New Approaches and Non-Incremental Methods of Calculation"* Springer Verlag, 1999.

[19] S. Ghosh, K. Lee and P. Raghavan, *"A multi-level computational model for multi-scale damage analysis in composite and porous materials"*, International Journal of Solids and Structures, 38, 2335-2385, 2001